Photon-Instanton Collider Implemented by a Superconducting Circuit

Amir Burshtein, Roman Kuzmin, Vladimir E. Manucharyan, and Moshe Goldstein

Phys. Rev. Lett. **126**, 137701 — Published 29 March 2021

DOI: 10.1103/PhysRevLett.126.137701

Photon-instanton collider implemented by a superconducting circuit

Amir Burshtein,[1] Roman Kuzmin,[2] Vladimir E. Manucharyan,[2] and Moshe Goldstein[1]

[1] *Raymond and Beverly Sackler School of Physics and Astronomy, Tel Aviv University, Tel Aviv 6997801, Israel*
[2] *Department of Physics, University of Maryland, College Park, MD 20742, USA*

Instantons, spacetime-localized quantum field tunneling events, are ubiquitous in correlated condensed matter and high energy systems. However, their direct observation through collisions with conventional particles has not been considered possible. We show how recent advance in circuit quantum electrodynamics, specifically, the realization of galvanic coupling of a transmon qubit to a high-impedance transmission line, allows the observation of inelastic collisions of single microwave photons with instantons (phase slips). We develop a formalism for calculating the photon-instanton cross section, which should be useful in other quantum field theoretical contexts. In particular, we show that the inelastic scattering probability can significantly exceed the effect of conventional Josephson quartic anharmonicity, and reach order-unity values.

Introduction.— Instantons are time-localized solutions to a system's imaginary time equations of motion, describing quantum tunneling events. They typically bridge between symmetry-related configurations and carry nontrivial topological indexes [1]. Instantons play important roles in many areas of physics, ranging from single-particle quantum-mechanical tunneling [1], through transport in low dimensional superconductors and superfluids (where they are also known as "phase slips", and can be thought of as vortices crossing the system) [2–9], to determining the phase diagram [10] and breaking of classical conservation laws [11, 12] in gauge theories. Most of these studies concern thermodynamic or transport properties. A more direct way to probe such short-lived excitations would be through resonances they may induce in the scattering cross sections or decay rates of other more stable particles with which they interact. However, such questions received much less attention, in large part due to lack of relevant experiments.

Advances in the fabrication and control of superconducting circuits allow to monitor the dynamics of single microwave photons. For example, recent experiments have exposed unusual relaxation dynamics in a uniform Josephson junction array, in which phase slips play an important role [13]. However, their interpretation is complicated due to the presence of disorder and offset charge fluctuations [14–16]. It has recently been realized theoretically [17–27] that controllable quantum simulation of many-body physics may be easier to achieve in "quantum impurity" setups, leading to initial experiments [28–32]. We thus study a single flux-tunable small Josephson junction in the regime where the Josephson energy still dominates (transmon qubit [33]), galvanically coupled to an array of large junctions. The array acts as a transmission line allowing microwave photons to controllably scatter off the small junction [30]. The large Josephson inductance makes the line wave impedance of the order of the resistance quantum, hence the array screens the effects of unwanted offset charges on the transmon without completely suppressing phase slips there. From a broader perspective, the large impedance amounts to an effective fine-structure constant of order unity [34], ushering in unprecedentedly strong correlations. We will show that a single photon propagating along the array may excite a phase slip at the transmon and inelastically convert into lower-frequency photons with a high probability, significantly larger than the conversion probability due to the usual Josephson quartic nonlinearity [35]; this effect could be measured via the resulting broadening of the array modes [13]. For this we develop an extension of the standard equilibrium instanton calculation [1] to a scattering scenario, which could be useful in other fields. We will now outline its main ingredients, deferring some technical details to the supplemental material [38].

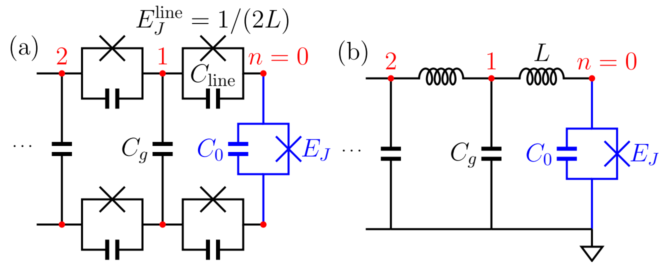

FIG. 1. The studied system: (a) The full circuit; (b) A simplified version. See the text for details.

Model.— We concentrate on the setup realized in a recent experiments [30, 39], corresponding to the electric circuit depicted in Fig. 1(a). It consists of a long (length $N \gg 1$) two-leg array of superconducting islands connected by strong Josephson junctions $E_J^{\rm line}$ with large junction capacitance $C^{\rm line}$, negligible ground capacitance (not depicted), and intermediate inter-leg capacitance C_g. The large $C^{\rm line}$ suppresses phase slips along the arrays, allowing their treatment as classical transmission lines. Except for this, $C^{\rm line}$ could be ignored below the array plasma frequency. The small ground capacitance pushes the leg-even modes to high frequencies, decoupling them from the transmon. We may thus employ a simplified single-leg array model [Fig. 1(b)] for the leg-odd degrees of freedom. The array capacitance to the ground C_g and inductance L in Fig. 1(b) are the inter-leg capacitance and twice the intra-leg Josephson inductance in Fig. 1(a), leading to a Lagrangian

$$\mathcal{L} = \frac{C_0\dot{\phi}_0^2}{2} + E_J \cos(2\phi_0) + \sum_{n=1}^{N} \frac{C_g\dot{\phi}_n^2}{2} - \frac{(\phi_n - \phi_{n-1})^2}{2L}, \quad (1)$$

where ϕ_n is in units of flux and we employ units where $e = 1$ and $\hbar = 1$, hence the flux quantum is $\Phi_0 = h/2e = \pi$. The array spacing a will serve as the unit of length.

The array is terminated by a transmon qubit [33] (node $n = 0$, blue elements in Fig. 1), a small SQUID whose Josephson energy E_J is flux-tunable and much larger than its charging energy, $E_C = 1/2C_0$. Hence, to leading order we may approximate its Josephson cosine by a quadratic function [30]. Then Eq. (1) gives rise to eigenmodes with dispersion $\omega_k = 2v\sin(k/2) \approx vk$, where $v = 1/\sqrt{LC_g}$, the array wave velocity divided by the array spacing, is much larger than all other energy scales, i.e., for all relevant modes $k \ll \pi$. The eigenmodes are $\propto \sin(kn + \delta_k)$, where [38, Sec. SI.B]

$$\delta_k = \tan^{-1}\left(\frac{\Gamma_0\omega_k}{\omega_0^2 - \omega_k^2}\right) \quad (2)$$

is the phase shift. Here $\omega_0 = \sqrt{8E_JE_C}$ is the trasmon LC frequency and $\Gamma_0 = 1/ZC_0 = 4E_C/\pi z$ is its elastic broadening due to its coupling to the array, where $Z = \sqrt{L/C_g}$ is the array wave impedance and $z = Z/R_Q$ ($R_Q = h/(2e)^2 = \pi/2$ is the superconducting resistance quantum). For $N \gg 1$ the mode spacing is $\Delta = \pi v/N$, hence $\sum_k \to \int_0^\infty \mathrm{d}\omega/\Delta$.

Upon increasing E_C/E_J the transmon nonlinearity starts becoming significant. We will concentrate on the regime where $\sqrt{E_C/E_J}$ is still small, and furthermore, $\Gamma_0/\omega_0 \ll 1$ (i.e., $\sqrt{E_C/E_J} \ll z$), so the transmon resonance is well-defined [30]. In this regime the nonlinearity manifests in two ways: (i) Expanding the Josephson cosine gives rise to quartic nonlinearity, shifting ω_0 by $-E_C$. It could also induce photon inelastic scattering, but we will show later on that for realistic device parameters this effect could be subleading; (ii) The periodicity of the cosine allows for instantons (phase slips). An incoming photon may excite a phase slip, and the resulting voltage and current pulse may give rise to the emission of photons with different frequencies. We will now study in detail the latter inelastic effect.

Instanton calculation.— For a disconnected transmon [first two terms of Eq. (1)] the classical instanton solution in imaginary time, describing a phase slip between $\phi_0(\tau \to -\infty) = 0$ and $\phi_0(\tau \to \infty) = \pm\Phi_0 = \pm\pi$, is $\phi_0^{(0)}(\tau) = \pm 2\tan^{-1}(e^{\omega_0\tau})$, or, in Fourier space, $\phi_0^{(0)}(\omega) = \pm\pi/i\omega\cosh(\pi\omega/2\omega_0)$ [1]. Here and below, the upper (lower) sign corresponds to an instanton (anti-instanton). The classical action S_0 of the instanton, together with the contributions of Gaussian fluctuations around it, give rise to the transmon ground state charge dispersion λ_0 (half the width of the lowest Bloch band of the corresponding Mathieu equation [33, 40]) in the WKB approximation [38, Sec. SI.A],

$$\lambda_0 \approx \frac{8}{\sqrt{\pi}}\left(8E_J^3E_C\right)^{1/4} e^{-\sqrt{8E_J/E_C}}. \quad (3)$$

We now incorporate the array to lowest order in Γ_0/ω_0. Expanding the imaginary time action around the classical isolated instanton solution [$\phi_0^{(0)}(\tau)$ as given above and $\phi_{n>0}^{(0)}(\tau) = 0$] to second order in the deviation $\delta\phi_n = \sum_k \delta\phi_k \sin(kn + \delta_k)$, one finds [38, Sec. SI.B]:

$$S = S_0 + \int \frac{\mathrm{d}\omega}{2\pi}\left[\frac{\left|\phi_0^{(0)}(\omega)\right|^2}{2L} + \sum_k \frac{C_k}{2}(\omega^2 + \omega_k^2)\left|\delta\phi_k(\omega)\right|^2 - \frac{\sin(k+\delta_k) - \sin(\delta_k)}{L}\phi_0^{(0)}(-\omega)\delta\phi_k(\omega)\right] - \int \mathrm{d}\tau \frac{8E_J}{\cosh^2(\omega_0\tau)}\left[\sum_k \sin(\delta_k)\delta\phi_k(\tau)\right]^2, \quad (4)$$

where the capacitance of mode k is $C_k \approx NC_g/2$ for $N \gg 1$. The very last term contributes to higher orders in Γ_0/ω_0 and will be neglected henceforth. The classical equations of motion for $\delta\phi_k$ result in

$$\delta\phi_k(\omega) \approx \frac{1}{C_k(\omega^2 + \omega_k^2)}\frac{\omega_k\cos\delta_k}{Z}\phi_0^{(0)}(\omega), \quad (5)$$

to leading order in $k \ll 1$. Plugging this back into the action [41] gives [38, Sec. SI.B]

$$\delta S = \frac{1}{2}\sum_k \tilde{f}_k^2, \quad \tilde{f}_k = \sqrt{\frac{2\Delta}{z\omega_k}}\frac{1}{\cosh\left(\frac{\pi}{2}\frac{\omega_k}{\omega_0}\right)}, \quad (6)$$

leading to a renormalization $\lambda_0 \to \lambda_0 e^{-\sum_k \tilde{f}_k^2/2}$. For $z > 1$ instantons are relevant, resulting in an emergent scale, $\lambda_* \sim \lambda_0(\lambda_0/\omega_0)^{1/(z-1)}$, below which instanton effects are nonperturbative [2]; we limit ourselves to higher energies.

Within the approximations we employ, the contribution of a single instanton to a multipoint correlation of the ϕ_k is given by the corresponding classical solution [41], multiplied by $\lambda_0 e^{-\sum_k \tilde{f}_k^2/2}/2$. By the LSZ reduction formula [42, 43], this correlation with its external single-particle legs amputated gives the $\mathcal{T}$-matrix element between N_{in} incoming photons with momenta $k'_1, k'_2, \cdots, k'_{N_{\text{in}}}$ and N_{out} outgoing photons with momenta $k_1, k_2, \cdots, k_{N_{\text{out}}}$ [38, Sec. SI.C]:

$$\mathcal{T}^{k_1',k_2',\cdots,k_{N_{\rm in}}'}_{k_1,k_2,\cdots,k_{N_{\rm out}}} = \frac{\Delta}{2\pi} \lim_{\substack{\{\omega_j'\to i\omega_{k_j'}\}\\ \{\omega_j\to -i\omega_{k_j}\}}} \prod_{j=1}^{N_{\rm in}} \frac{C_{k_j'}\left(\omega_j'^2+\omega_{k_j'}^2\right)}{\sqrt{2C_{k_j'}\omega_{k_j'}}} \prod_{j=1}^{N_{\rm out}} \frac{C_{k_j}\left(\omega_j^2+\omega_{k_j}^2\right)}{\sqrt{2C_{k_j}\omega_{k_j}}} \left\langle \prod_{j=1}^{N_{\rm in}} \phi_{k_j'}(\omega_j') \prod_{j=1}^{N_{\rm out}} \phi_{k_j}(\omega_j) \right\rangle_{1-\rm instanton}$$
$$= (\mp 1)^{N_{\rm in}} (\pm 1)^{N_{\rm out}} f_{k_1'} f_{k_2'} \cdots f_{k_{N_{\rm in}}'} f_{k_1} f_{k_2} \cdots f_{k_{N_{\rm out}}} \frac{\lambda_0}{2} e^{-\sum_k \tilde{f}_k^2/2} \quad (7)$$

with

$$f_k = \sqrt{\frac{2\Delta}{z\omega_k}} \frac{\omega_0^2-\omega_k^2}{\sin\left(\frac{\pi}{2}\frac{\omega_0-\omega_k}{\omega_0}\right)\sqrt{\left(\omega_0^2-\omega_k^2\right)^2+(\Gamma_0\omega_k)^2}}, \quad (8)$$

being the "form factor" of the instanton in the photon modes basis. Note that it is finite at the resonance frequency ω_0 but still peaked there. It rises towards low frequencies (assumed higher than λ_*); this reflects the fact that an instanton involves a shift of phases along the entire array, hence couples well to low-k modes. Thus, processes in which a nearly resonant photon scatters into one nearly resonant photon and several low energy photons (whose number is controlled by z) will play an important role. Note also that f_k diverges at higher odd multiples of ω_0, which are nonlinear resonances broadened only at higher order in Γ_0. In relevant experiments [30] these will anyway be close to E_J, i.e., outside the instanton regime, hence we will limit ourselves here to lower frequencies. Adding up the contribution of the instantons and the anti-instantons eliminates processes involving an odd number of photons.

Let us consider processes in which an additional photon with the specific frequency ω_k is included among either the incoming or outgoing photons. Combining the square of the $\mathcal{T}$-matrix elements just obtained with the appropriate Bose-Einstein factors corresponding to spontaneous and stimulated emission as well as stimulated absorption, gives the total rate $\Gamma_k^{\rm in}$ of the inelastic decay (minus creation) of a single incoming photon at k [38, Sec. SI.D] (the inelastic scattering probability per collision is $2\pi\Gamma_k^{\rm in}/\Delta$, while $\omega_k/\Gamma_k^{\rm in}$ is the experimentally-measurable quality factor of mode k [30]) [44],

$$\Gamma_k^{\rm in} = \frac{\lambda_0^2}{2} f_k^2 e^{-\sum_{k'}\tilde{f}_{k'}^2 - 2\sum_{k'} f_{k'}^2 n_B(\omega_{k'})} \sum_{N_{\rm out},N_{\rm in}} \sum_{\substack{k_1<\cdots<k_{N_{\rm out}},\\ k_1'<\cdots<k_{N_{\rm in}}'}} f_{k_1}^2\cdots f_{k_{N_{\rm out}}}^2 f_{k_1'}^2\cdots f_{k_{N_{\rm in}}'}^2 (1+n_B(\omega_{k_1}))\cdots(1+n_B(\omega_{k_{N_{\rm out}}}))\times$$
$$n_B(\omega_{k_1'})\cdots n_B(\omega_{k_{N_{\rm in}}'}) 2\pi\left[\delta\left(\omega_k+\omega_{k_1'}+\cdots+\omega_{k_{N_{\rm in}}'}-\omega_{k_1}-\cdots-\omega_{k_{N_{\rm out}}}\right)-\{\omega_k\to-\omega_k\}\right], \quad (9)$$

The probability of a process not involving photons with frequency $\omega_{k'}$ decreases when such photons are present, due to the increased probability of their emission or absorption. This is accounted for by the factor $e^{-2\sum_{k'} f_{k'}^2 n_B(\omega_{k'})}$ [38, Sec. SI.D].

Upon expressing the delta functions via their Fourier representations, the summations over $N_{\rm in,out}$ and the ks can be recognized as the Taylor series of an exponent. All in all we find that $\Gamma_k^{\rm in} = 2f_k^2 \Im\Pi_R(\omega_k)$, where

$$\Pi_R(\omega) = -\lambda_0^2 \int_0^\infty {\rm d}t \sin(\omega t) \exp\left(-\sum_{k'}\left\{f_{k'}^2\left[(1+n_B(\omega_{k'}))(1-e^{-i\omega_{k'}t})+n_B(\omega_{k'})(1-e^{i\omega_{k'}t})\right]+\tilde{f}_{k'}^2-f_{k'}^2\right\}\right), \quad (10)$$

is the photon retarded self energy, whose imaginary part gives the total inelastic conversion (absorption minus emission) rate of energy ω into any photon combination. Using it, one may write down more refined rates; for example, the net rate of creation of photons at k' due to processes involving an incoming photon at k is

$$\Gamma_{k'|k}^{\rm in} = 2f_k^2 f_{k'}^2 \left\{\Im\Pi_R(\omega_k-\omega_{k'})\left[(1+n_B(\omega_{k'}))(1+n_B(\omega_k-\omega_{k'}))-n_B(\omega_{k'})n_B(\omega_k-\omega_{k'})\right]\right.$$
$$\left.+\Im\Pi_R(\omega_k+\omega_{k'})\left[(1+n_B(\omega_{k'}))n_B(\omega_k+\omega_{k'})-n_B(\omega_{k'})(1+n_B(\omega_k+\omega_{k'}))\right]\right\}, \quad (11)$$

which accounts for processes in which photons at k, k' are, respectively, absorbed-emitted, emitted-absorbed,

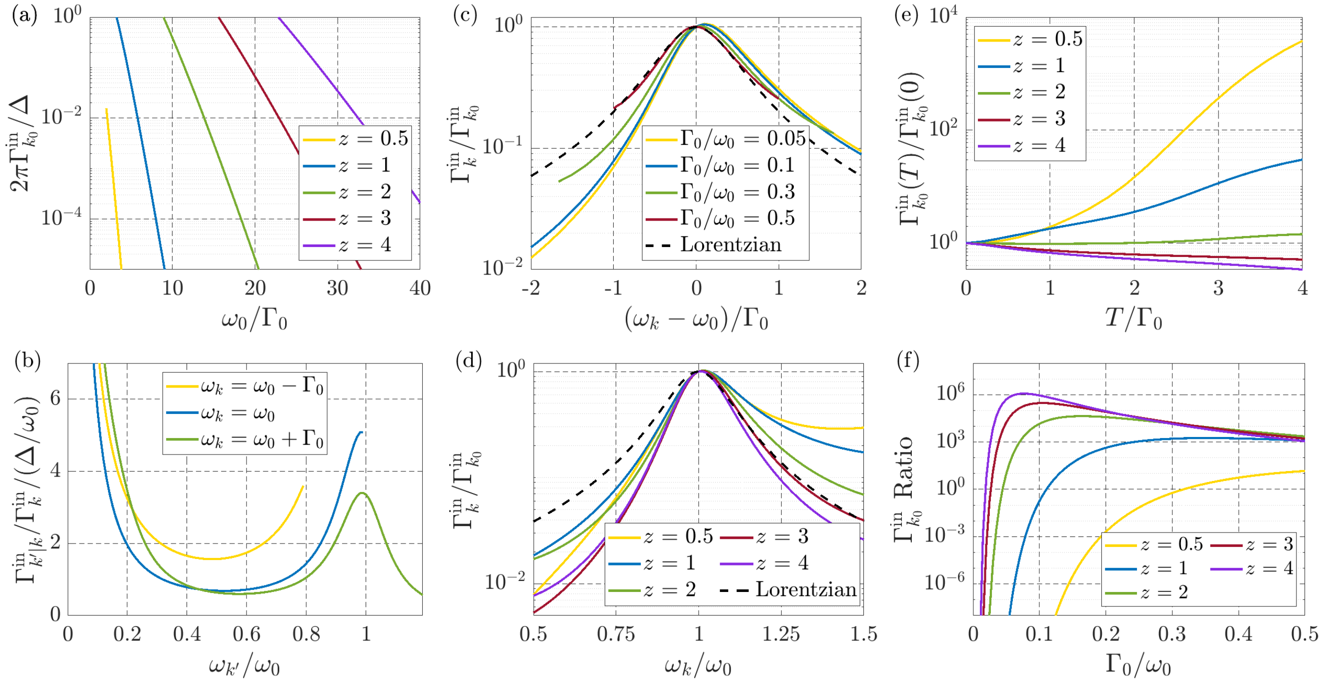

FIG. 2. Parameter dependence of the inelastic scattering probability of a single incoming photon with frequency ω_k by a single phase slip, Eqs. (10)–(11). (a) On-resonance (mode $k_0 = \omega_0/v$) total probability $2\pi\Gamma^{\rm in}_{k_0}/\Delta$ as function of ω_0/Γ_0 for several values of z at $T = 0$ {using the full Mathieu expression for λ_0 [33, 40], rather than the approximate Eq. (3) [38, Sec. SI.A]}. (b) The distribution of inelastically generated photons $\Gamma^{\rm in}_{k'|k}/\Gamma^{\rm in}_k$ at $\omega_k = \omega_0, \omega_0 \pm \Gamma_0$ for $z = 2$ and $\Gamma_0/\omega_0 = 0.2$. (c,d) $T = 0$ resonance lineshape at (c) $z = 2$ and different Γ_0/ω_0 or (d) $\Gamma_0/\omega_0 = 0.2$ and different z. A simple Lorentzian with width Γ_0 is also plotted for comparison. (e) Temperature dependence of the on-resonance probability for $\Gamma_0/\omega_0 = 0.05$ and different z. (f) Ratio between the $T = 0$ on-resonance probabilities due to the instantons and due to the quatric nonlinearity, Eq. (16), showing that the former may dominate by several orders of magnitude for not-too-small Γ_0/ω_0 and $z \gtrsim 1$.

emitted-emitted, or absorbed-absorbed, with appropriate signs to obey an energy conservation sum rule, $\omega_k\Gamma^{\rm in}_k = \sum_{k'}\omega_{k'}\Gamma^{\rm in}_{k'|k}$. The last couple of equations are the central results of this work. To recap, they apply for any $\omega_k, \omega_{k'}$ between λ_* and $3\omega_0$, provided that $\lambda_* \ll \max(\Gamma_0, T) \ll \omega_0$ and $E_C \ll E_J$. The single-instanton approximation further requires $2\pi\Gamma^{\rm in}_k/\Delta \lesssim 1$.

Inelastic rate behavior.— We exemplify the parameter dependence of the inelastic rate in Fig. 2. To better understand its behavior, it is useful to study some limits [38, Sec. SI.E]. First, at $T = 0$ and low frequencies $\omega \ll \omega_0$ one may approximate $f_q \approx\sim \sqrt{2\Delta/z\omega_q}$ in Eq. (10), leading to [45]

$$\Pi_R(\omega) \approx \frac{\pi}{\Gamma(2/z)}\frac{\lambda_0^2}{\omega}\left(\frac{\omega}{\omega_c(z)}\right)^{2/z}, \tag{12}$$

where $\Gamma(x)$ is the gamma function [40], and the effective cutoff $\omega_c(z) \approx 0.9\omega_0$ is z independent for $z \gtrsim 1$.

Let us now turn to the scattering of nearly-resonant photons, $\omega \approx \omega_k$, starting with $T = 0$. As the spectrum of inelastically-emitted photons in Fig. 2(b) exemplifies, for $z \gtrsim 1$ and $\Gamma_0/\omega_0 \to 0$ the dominant process involves one emitted photon at $\omega'_k \approx \omega_k$, while the other photons carry low energy of order Γ_0, hence

$$\frac{2\pi\Gamma^{\rm in}_{k'|k}}{\Delta^2} \approx \frac{2\lambda_1^2}{\Gamma(2/z)\omega_c}\left(\frac{\omega_k - \omega_{k'}}{\omega_c}\right)^{\frac{2-z}{z}} \prod_{q=k,k'} \frac{\frac{\Gamma_0}{2}}{(\omega_0 - \omega_q)^2 + \left(\frac{\Gamma_0}{2}\right)^2}, \tag{13}$$

where $\lambda_1 = -\sqrt{2^7 E_J/E_C}\lambda_0$ is the charge dispersion of the first excited level of an isolated transmon [33]. Summing over k' one obtains on resonance (mode $k_0 = \omega_0/v$),

$$\frac{2\pi\Gamma^{\rm in}_{k_0}}{\Delta} \approx \frac{\pi(\omega_0/\omega_c)^{2/z}}{\Gamma(2/z)\sin(\pi/z)}\frac{\lambda_1^2}{(\Gamma_0/2)^2}\left(\frac{\Gamma_0/2}{\omega_0}\right)^{2/z}. \tag{14}$$

The charge dispersion λ_0 decreases fast with ω_0, masking the corresponding increase in the number of possible decay channels contributing on-resonance [Fig. 2(a)]; this serves to distinguish this processes from parasitic effects, such as dielectric loss, which display the opposite behavior [13]. We further see that the inelastic scattering probability can approach order unity in the recently-achieved regime of effective fine-structure constant $z \gtrsim 1$ [13, 30, 46]. The increase in number of channels with frequency is seen in an asymmetry of the inelastic resonance lineshape [Fig. 2(c,d)]; For $|\omega_k - \omega_0| \ll \omega_0$

one has

$$\frac{\Gamma_k^{\text{in}}}{\Gamma_{k_0}^{\text{in}}} \approx \begin{cases} 2\sin\left(\frac{\pi}{z}\right)\left(\frac{\Gamma_0/2}{\omega_k-\omega_0}\right)^{3-2/z}, & \omega_k-\omega_0 \gg \Gamma_0, \\ \frac{(\Gamma_0/2)^2}{(\omega_0-\omega_k)^2+(\Gamma_0/2)^2}, & |\omega_k-\omega_0| \lesssim \Gamma_0, \\ \frac{1-2/z}{\cos(\pi/z)}\left(\frac{\Gamma_0/2}{\omega_0-\omega_k}\right)^{4-2/z}, & \omega_0-\omega_k \gg \Gamma_0. \end{cases} \quad (15)$$

Finally, let us note that temperature suppresses coherent quantum phase slips (particularly for $z > 1$, when they are relevant [2]) but gives rise to scattering by thermal photons, hence could either decrease or increase the decay rate, depending on z, as shown in Fig. 2(e). Similar expressions to Eqs. (13)–(15) can be obtained via an effective Hamiltonian tailored to describe this particular class of processes [47], though that approach cannot give the value of ω_c.

Quartic nonlinearity.— Let us now briefly discuss inelastic photon scattering by more mundane nonlinearities, coming from the Taylor expansion of the transmon Josephson cosine. To leading order in $\sqrt{E_C/E_J}$ it is dominated by the Fermi golden rule contribution of the quartic term in the expansion, which at $T = 0$ allows an incoming photon at k to split into three at k_i, $i = 1, 2, 3$. Expressing ϕ_0 in terms of the array modes, one finds [38, Sec. SIII]

$$\Gamma_k^{\text{in}} = \frac{4z^2}{3\pi}\frac{\omega_0^4\Delta^4}{\Gamma_0^2}\frac{\sin^2(\delta_k)}{\omega_k}\sum_{k_i}\frac{\sin^2(\delta_{k_1})}{\omega_{k_1}}\times \frac{\sin^2(\delta_{k_2})}{\omega_{k_2}}\frac{\sin^2(\delta_{k_3})}{\omega_{k_3}}\delta(\omega_k-\omega_{k_1}-\omega_{k_2}-\omega_{k_3}). \quad (16)$$

As opposed to the instanton contribution, where f_k^2 increases towards low energies [Eq. (8)], here the factors $\sin^2(\delta_{k_i})/\omega_{k_i} \propto \omega_{k_i}$ [cf. Eq. (2)] suppress the contribution of low frequency photons, and severely limit the phase space for splitting of nearly-resonant photons. Summing over k_i we find the resulting total inelastic rate near resonance to scale as $\sim z^2\Delta\Gamma_0^4/\omega_0^4$. The suppression with Γ_0/ω_0 can make it significantly smaller than the instanton contribution, provided λ_1 is not too small [cf. Eq. (14)]. The ratio between the corresponding rates is depicted in Fig. 2(f), which shows that instanton processes are stronger by several orders of magnitude in the experimentally-accessible regime of not-too-small Γ_0/ω_0 and $z \gtrsim 1$ [where the exponential factor in Eq. (3) does not dominate] [30].

Conclusions.— In this work we have developed a general formalism for the study of instanton-particle collisions, and applied it to a recently-realized [30] superconducting circuit in which a transmon qubit is strongly-coupled to a high impedance transmission line. We have shown that significant inelastic single-photon scattering by instantons can be controllably initiated and identified in such a setup: As opposed to the Josephson quartic nonlinearity, which only affects near-resonance photons and thus cannot split them into low frequency ones, an instanton shifts the phases along the entire array, hence couples well to low-k modes, and allows a near-resonant incoming photon to dissipate energy into them. An experiment has now appeared [39] demonstrating this effect, with favorable comparison to a simplified version of our theory [38, Sec. SII]. This paves the way towards the study of similar effects not only in various superconducting circuits [2, 3, 5–9, 17–29, 31, 32], but also in other condensed matter (e.g., atomtronic setups) [4, 48, 49] and particle physics [10–12] systems.

We thank L.I. Glazman and M. Houzet for very useful discussions and for sharing with us their unpublished results [47]. Our work has been supported by the U.S.-Israel Binational Science Foundation (Grants No. 2014262 and 2016224). V.E.M. was further supported by a US DOE Early Career Award, and M.G. by the Israel Science Foundation (Grant No. 227/15).

[1] M. Mariño, *Instantons and Large N: An Introduction to Non-Perturbative Methods in Quantum Field Theory* (Cambridge University Press, Cambridge, UK, 2015).

[2] G. Schön and A. D. Zaikin, Quantum coherent effects, phase transitions, and the dissipative dynamics of ultra small tunnel junctions, Physics Reports **198**, 237 (1990).

[3] R. Fazio and H. van der Zant, Quantum phase transitions and vortex dynamics in superconducting networks, Physics Reports **355**, 235 (2001).

[4] A. J. Leggett, *Quantum Liquids* (Oxford University Press, Oxford, UK, 2006).

[5] A. M. Hriscu and Y. V. Nazarov, Model of a proposed superconducting phase slip oscillator: A method for obtaining few-photon nonlinearities, Phys. Rev. Lett. **106**, 077004 (2011).

[6] G. Rastelli, I. M. Pop, and F. W. J. Hekking, Quantum phase slips in Josephson junction rings, Phys. Rev. B **87**, 174513 (2013).

[7] A. Ergül, J. Lidmar, J. Johansson, Y. Azizoğlu, D. Schaeffer, and D. B. Haviland, Localizing quantum phase slips in one-dimensional Josephson junction chains, New Journal of Physics **15**, 095014 (2013).

[8] N. Vogt, J. H. Cole, and A. Shnirman, De-pinning of disordered bosonic chains, New Journal of Physics **18**, 053026 (2016).

[9] M. Bard, I. V. Protopopov, I. V. Gornyi, A. Shnirman, and A. D. Mirlin, Superconductor-insulator transition in disordered Josephson-junction chains, Phys. Rev. B **96**, 064514 (2017).

[10] A. M. Polyakov, *Gauge Fields and Strings* (Harwood, Chur, Switzerland, 1987).

[11] S. Coleman, The uses of instantons, in *The Whys of Subnuclear Physics*, edited by A. Zichichi (Springer, Boston, 1979).

[12] D. J. Gross, R. D. Pisarski, and L. G. Yaffe, QCD and instantons at finite temperature, Rev. Mod. Phys. **53**, 43 (1981).

[13] R. Kuzmin, R. Mencia, N. Grabon, N. Mehta, Y.-H. Lin, and V. E. Manucharyan, Quantum electrodynamics of a superconductorinsulator phase transition, Nature

Physics **15**, 930 (2019).
[14] M. Bard, I. V. Protopopov, and A. D. Mirlin, Decay of plasmonic waves in Josephson junction chains, Phys. Rev. B **98**, 224513 (2018).
[15] M. Houzet and L. I. Glazman, Microwave spectroscopy of a weakly pinned charge density wave in a superinductor, Phys. Rev. Lett. **122**, 237701 (2019).
[16] H.-K. Wu and J. D. Sau, Theory of coherent phase modes in insulating Josephson junction chains, Phys. Rev. B **99**, 214509 (2019).
[17] S. Camalet, J. Schriefl, P. Degiovanni, and F. Delduc, Quantum impurity approach to a coupled qubit problem, Europhysics Letters (EPL) **68**, 37 (2004).
[18] J. J. García-Ripoll, E. Solano, and M. A. Martin-Delgado, Quantum simulation of Anderson and Kondo lattices with superconducting qubits, Phys. Rev. B **77**, 024522 (2008).
[19] K. Le Hur, Kondo resonance of a microwave photon, Phys. Rev. B **85**, 140506(R) (2012).
[20] M. Goldstein, M. H. Devoret, M. Houzet, and L. I. Glazman, Inelastic microwave photon scattering off a quantum impurity in a Josephson-junction array, Phys. Rev. Lett. **110**, 017002 (2013).
[21] B. Peropadre, D. Zueco, D. Porras, and J. J. García-Ripoll, Nonequilibrium and nonperturbative dynamics of ultrastrong coupling in open lines, Phys. Rev. Lett. **111**, 243602 (2013).
[22] I. Snyman and S. Florens, Robust Josephson-Kondo screening cloud in circuit quantum electrodynamics, Phys. Rev. B **92**, 085131 (2015).
[23] N. Gheeraert, S. Bera, and S. Florens, Spontaneous emission of Schrdinger cats in a waveguide at ultrastrong coupling, New Journal of Physics **19**, 023036 (2017).
[24] J. Leppäkangas, J. Braumüller, M. Hauck, J.-M. Reiner, I. Schwenk, S. Zanker, L. Fritz, A. V. Ustinov, M. Weides, and M. Marthaler, Quantum simulation of the spin-boson model with a microwave circuit, Phys. Rev. A **97**, 052321 (2018).
[25] N. Gheeraert, X. H. H. Zhang, T. Sépulcre, S. Bera, N. Roch, H. U. Baranger, and S. Florens, Particle production in ultrastrong-coupling waveguide qed, Phys. Rev. A **98**, 043816 (2018).
[26] T. Yamamoto and T. Kato, Microwave scattering in the subohmic spin-boson systems of superconducting circuits, Journal of the Physical Society of Japan **88**, 094601 (2019).
[27] R. Belyansky, S. Whitsitt, R. Lundgren, Y. Wang, A. Vrajitoarea, A. A. Houck, and A. V. Gorshkov, Transport and dynamics in the frustrated two-bath spin-boson model, arXiv:2007.03690 [quant-ph] (2020).
[28] P. Forn-Díaz, J. García-Ripoll, B. Peropadre, J.-L. Orgiazzi, M. Yurtalan, R. Belyansky, C. Wilson, and A. Lupascu, Ultrastrong coupling of a single artificial atom toan electromagnetic continuum in the nonperturbative regime, Nature Physics **13**, 39 (2017).
[29] L. Magazzù, P. Forn-Díaz, R. Belyansky, J.-L. Orgiazzi, M. A. Yurtalan, M. R. Otto, A. Lupascu, C. M. Wilson, and M. Grifoni, Probing the strongly driven spin-boson model in a superconducting quantum circuit, Nature Communications **9**, 1403 (2018).
[30] R. Kuzmin, N. Mehta, N. Grabon, R. Mencia, and V. E. Manucharyan, Superstrong coupling in circuit quantum electrodynamics, npj Quantum Information **5**, 1 (2019).
[31] J. Puertas Martínez, S. Léger, N. Gheeraert, R. Dassonneville, L. Planat, F. Foroughi, Y. Krupko, O. Buisson, C. Naud, W. Hasch-Guichard, S. Florens, I. Snyman, and N. Roch, A tunable Josephson platform to explore many-body quantum optics in circuit-QED, npj Quantum Information **5**, 19 (2019).
[32] S. Indrajeet, H. Wang, M. D. Hutchings, B. G. Taketani, F. K. Wilhelm, M. D. LaHaye, and B. L. T. Plourde, Coupling a superconducting qubit to a left-handed metamaterial resonator, arXiv:2007.10932 [quant-ph] (2020).
[33] J. Koch, T. M. Yu, J. Gambetta, A. A. Houck, D. I. Schuster, J. Majer, A. Blais, M. H. Devoret, S. M. Girvin, and R. J. Schoelkopf, Charge-insensitive qubit design derived from the Cooper pair box, Phys. Rev. A **76**, 042319 (2007).
[34] V. E. Manucharyan, J. Koch, L. I. Glazman, and M. H. Devoret, Fluxonium: Single cooper-pair circuit free of charge offsets, Science **326**, 113 (2009).
[35] By the dynamical Coulomb blockade [36], inelastic Cooper pair tunneling (dual to phase slips) could also induce photon emission [37, and references therein]. However, that process is driven by a dc voltage bias, akin (by the ac Josephson effect) to strong pumping by a microwave source in our setup, in marked distinction from the single photon excitation regime we consider.
[36] G. L. Ingold and Y. V. Nazarov, Charge tunneling rates in ultrasmall junctions, in *Single Charge Tunneling*, NATO ASI Series B, Vol. 294, edited by H. Grabert and M. H. Devoret (Plenum, New York, 1992) pp. 21–107.
[37] A. Peugeot, G. Menárd, S. Dambach, M. Westig, B. Kubala, Y. Mukharsky, C. Altimiras, P. Joyez, D. Vion, P. Roche, D. Esteve, P. Milman, J. Leppäkangas, G. Johansson, M. Hofheinz, J. Ankerhold, and F. Portier, Generating two continuous entangled microwave beams using a dc-biased Josephson junction, arXiv:2010.03376 [cond-mat.mes-hall] (2020).
[38] See the supplemental material for further details of the derivations.
[39] R. Kuzmin, N. Grabon, N. Mehta, A. Burshtein, M. Goldstein, M. Houzet, L. I. Glazman, and V. E. Manucharyan, Photon decay in circuit quantum electrodynamics, arXiv:2010.02099 [cond-mat.supr-con] (2020).
[40] M. Abramowitz and I. A. Stegun, *Handbook of Mathematical Functions* (Dover, New York, 1965).
[41] Corrections to the fluctuations contribution are subleading in Γ_0/ω_0.
[42] M. E. Peskin and D. V. Schroeder, *An Introduction to Quantum Field Theory* (CRC Press, Boca Raton, 2015).
[43] J.-G. Zhou, J.-Q. Liang, J. Burzlaff, and H. Müller-Kirsten, Instanton induced tunneling amplitude at excited states with the LSZ method, Physics Letters A **224**, 142 (1996).
[44] The sum is restricted to odd $N_{\rm out}+N_{\rm in}\geq 3$. However, in the thermodynamic limit one may discard this restriction and introduce the prefactor of half [38, Sec. SI.D].
[45] A. O. Gogolin, A. A. Nersesyan, and A. M. Tsvelik, *Bosonization and strongly correlated systems* (Cambridge University Press, 2004).
[46] M. Devoret, S. Girvin, and R. Schoelkopf, Circuit-QED: How strong can the coupling between a Josephson junction atom and a transmission line resonator be?, Annalen der Physik **16**, 767 (2007).
[47] M. Houzet and L. I. Glazman, in preparation.
[48] C. L. Kane and M. P. A. Fisher, Transport in a one-channel luttinger liquid, Phys. Rev. Lett. **68**, 1220

(1992).
[49] S. Krinner, D. Stadler, D. Husmann, J.-P. Brantut, and T. Esslinger, Observation of quantized conductance in neutral matter, Nature **7532**, 64 (2015).